Structural properties of kinks and domain walls in nonlinear oscillatory lattices

Bruce Denardo[1] and William B. Wright[2]
[1]*Department of Physics and Astronomy, University of Mississippi, University, Mississippi 38677*
[2]*Department of Physics, University of California, Los Angeles, California 90024-1547*
(Received 14 July 1993; revised manuscript received 25 July 1994)

Structural properties of self-localized steady-state modes in damped parametrically driven lattices have been numerically observed. The states are *kinks,* which are localized regions between two standing wave domains of the same wave number with an offset in spatial phase; and *domain walls,* which are localized regions between two standing wave domains of different wave numbers. The properties include preferred definite symmetry, a wide variety of distinct states, and hysteretic transitions that occur along boundaries in the plane of the drive parameters (amplitude and frequency). The transitions of the localized states exhibit the spontaneous processes of symmetry reversal and "complexification," as well as the onset of quasiperiodicity and chaos. Simple plausible models based upon few degrees of freedom fail to correctly describe the instabilities, which indicates that the behavior is a collective phenomenon.

PACS number(s): 46.10.+z, 63.20.Pw, 63.20.Ry

I. INTRODUCTION

Nonlinearity can give rise to self-localized waves that have been observed in various systems. The classic example is the Korteweg–de Vries soliton, which was first observed in the nineteenth century [1]. The requirement that self-localized waves occur for free motion drastically restricts their existence. In particular, the inclusion of dissipation and parametric drive leads to a wealth of steady localized states in one-dimensional oscillatory lattices. In this article, we report numerical investigations of three such types of nonpropagating self-localized structures: cutoff kinks, noncutoff kinks, and domain walls. The kinks are localized regions between two standing wave domains of the same wave number with a mismatch in spatial phase, whereas the domain walls are localized regions between two standing wave domains of different wave number. In a previous article [2], we and our collaborators established the existence of these states in an actual pendulum lattice and a simple numerical model. In the present article, we numerically examine some of the structural properties of the localized states. These include states with preferred definite symmetry, a wide variety of states corresponding to different initial conditions and different spatial mismatches, and instabilities and resultant transitions that occur along boundaries in the plane of the drive parameters as these are slowly varied.

Steady-state kinks and breathers have been previously observed in *cutoff* standing wave modes which are at the extremes of the oscillation band, where the group velocity vanishes. These observations include lower cutoff surface wave kinks [3] and breathers [4], lower cutoff pendulum lattice breathers [5], upper cutoff pendulum lattice kinks [2], and upper cutoff magnetic lattice breathers [6]. Various approximate analytical treatments [2,3,5–10] of these states can be summarized and unified [5] by the fact that weakly-nonlinear slowly-varying amplitude modulations of cutoff modes yield a nonlinear Schrödinger equation that possesses kink (hyperbolic tangent) or breather (hyperbolic secant) solutions, depending upon whether the mode is lower or upper cutoff (sign of the dispersion) and whether the mode softens or hardens (sign of the nonlinear coefficient). In the case of no drive and dissipation, propagating solutions exist and are known to be solitons [11]. An important observation in our previous article [2] is that lattice kinks are not restricted to cutoff modes, but can occur in modes inside the oscillation band (noncutoff kinks). Furthermore, the wave number need not be the same on either side of a localized structure (domain walls). The straightforward amplitude modulation analysis which describes the cutoff solitons fails for noncutoff kinks and domain walls, and has prompted several theories [12–14]. As explained in Sec. V, our observations of domain walls conflicts with the continuum theory [13,14] of these states. The stability of noncutoff kinks and domain walls in undriven undamped (Hamiltonian) media is an open question.

The observations of upper cutoff kinks, noncutoff kinks, and domain walls are not restricted to our model equation (Sec. II) with a softening nonlinearity. We have also observed these structures in the hardening version of the equation, and with a quadratic rather than cubic nonlinearity, as well as in damped parametrically driven sine-Gordon and sinh-Gordon lattices. The robustness of these states suggests that they should be observable in many other systems, e.g., in (a) a damped parametrically driven ϕ^4 lattice, (b) lattices where the parametric drive operates through the coupling, and where there are no external potential wells, (c) higher-dimensional lattices, (d) continua, and (e) certain bimodal lattices. In (a), the localized states should exist in modes where all of the oscillators are on a common side of the double potential well. Various effects of damping and parametric drive on topological kinks in ϕ^4 and sine-Gordon lattices, which model many condensed matter systems, have recently been investigated [15,16]. A possibility in (b) is a damped parametrically driven Toda lattice, which should possess

nonpropagating breathers in the upper cutoff mode (as a result of the hardening), and may possess kinks in noncutoff modes and domain walls between different modes. This is interesting because the Toda lattice is integrable in the limit of no drive and dissipation, and the resultant solitons have no obvious connection with the driven damped breathers, noncutoff kinks, and domain walls. Regarding (e), for a localized state to be parametrically driven, it should be noted that the drive need not be external. In a system that supports several different types of waves (i.e., where the dispersion law is multivalued), one long-wavelength wave can act through nonlinearities as an effective global parametric drive on a short-wavelength wave of a different type. The localized waves reported here may thus have application to biological molecular chains, which typically have modes of various types (e.g., transverse and longitudinal modes, as in models of DNA [17]).

An interesting and potentially profound aspect of our observations pertains to *mesoscopic* phenomena, by which we mean the physics of systems whose number of active degrees of freedom are between a few and very many. For example, we find that the number of physically distinct modes of a lattice can easily exceed the number of degrees of freedom of the system. As other examples, we observe the phenomena of spontaneous symmetry reversal and "complexification," in which a localized structure spontaneously spawns a second localized structure that is bound to it. Furthermore, we show that the instabilities that occur in the localized structures cannot be successfully modeled by few-degree-of-freedom systems, even though these models are very plausible.

The model equation and our various numerical techniques are discussed in Sec. II. The basic features of cutoff kinks, noncutoff kinks, and domain walls are examined in Secs. III, IV, and V, respectively. Symmetry reversals, quasiperiodicity, and chaos are then examined in more detail in Sec. VI. Finally, in Sec. VII, several few-degree-of-freedom models of the instabilities are considered and compared to observations.

II. MODEL SYSTEM

Our system is a one-dimensional lattice of identical nonlinear oscillators that are linearly coupled. The nonlinearity is a simple cubic in the displacement, and the dissipation is linear. The linear part of the oscillator restoring force is modulated uniformly in space, which subjects the lattice to a global parametric drive. The equation of motion of the lattice is

$$\frac{d^2\theta_n}{dt^2}-c^2(\theta_{n+1}-2\theta_n+\theta_{n-1})+\beta\frac{d\theta_n}{dt}+[\omega_0^2+\eta\cos(2\omega t)]\theta_n=\alpha\theta_n^3 , \quad (1)$$

where θ_n is the displacement of the nth oscillator, ω_0 is the linear frequency of an uncoupled oscillator, η is the drive amplitude, 2ω is the drive frequency, β is the damping parameter, c^2 is a measure of the coupling strength, and α is the nonlinear coefficient. An actual system approximated by (1) is a vertically oscillated lattice of coupled pendulums whose amplitudes are not large [2], in which case $\alpha=\omega_0^2/6$. We choose a cubic nonlinearity because it is the simplest, and because we wish to show that the $\sin(\theta)$, which occurs in the equation of motion of the actual lattice and other systems, plays no essential role in the existence of the localized states. This nonlinearity is also advantageous because we can generalize the model by allowing α to be positive (softening system), zero (linear system), or negative (hardening system). By "softening" or "hardening" is meant that the frequency of a free standing wave decreases or increases, respectively, at greater amplitudes.

By scaling time and displacement, we can normalize ω_0 and the magnitude of α in the equation of motion (1). Without loss of generality, then, we choose $\omega_0=1$ and $\alpha=+1$, 0, or -1. Unless otherwise specified, the results presented here are for a softening system ($\alpha=+1$) with $c^2=0.1$ and $\beta=0.03$. The stability of all steady states was checked by perturbing the displacements near a turning point of the motion. Each oscillator was given a random perturbation between $\pm 5\%$ of the maximum amplitude in the lattice. Periodic boundary conditions yielded essentially the same results as "reflecting" boundary conditions, in which virtual oscillators next to the ends of the lattice are specified to have the same instantaneous displacements as the oscillators one wavelength minus one lattice spacing from the end. Our domain wall investigations were performed with reflecting boundary conditions, because in this case a single domain wall can occur in the lattice. Our kink investigations were performed with periodic boundary conditions.

If the number of oscillators does not exceed several hundred, the numerical solution of (1) can be handled on a fast personal computer with a simple finite-difference method. The fourth-order Runge-Kutta method is employed here. We developed the software to be highly interactive and visual, with the instantaneous displacements displayed graphically on a monitor, so the user could observe the evolution as a result of either the initial conditions or changes in the values of the drive parameters. These capabilities are very advantageous in the observation and investigation of the localized states. Many analysis features were implemented in order to conveniently probe the system during the motion. These consisted of menu-driven "windows" that would display various quantities, including the amplitude and phase of an oscillator selected by the user, as well as a Poincaré map and fast-Fourier spectrum. Any display, particularly the instantaneous displacements of the oscillators, could be temporarily turned off in order to increase the speed of the simulations.

III. UPPER CUTOFF KINKS

The simplest kinks reported here are those that occur in a standing *cutoff* mode of a lattice, provided that the mode is stable at finite amplitudes. For a softening lattice, the upper cutoff mode is stable and can possess kinks. The lower cutoff mode is subject to the Benjamin-Feir instability [5,18], and the motion evolves into breather solitons. For a hardening lattice, the behavior

of the upper and lower cutoff modes is reversed. Numerical simulations of (1) show that stable steady-state kinks can indeed exist in the upper cutoff mode of a softening ($\alpha>0$) lattice and in the lower cutoff mode of a hardening ($\alpha<0$) lattice. In this article, we focus on the upper cutoff kinks. For most of the region in the drive parameter space in which these kinks exist (see below), only states with definite symmetry are stable. Figure 1 shows the oscillators' displacements at turning points of the motion, for the cases of small and large amplitude kinks in the upper cutoff mode. In Fig. 2, the kink structures are more clearly and compactly displayed by the diagrammatic representations of the highly localized (large-amplitude) states.

Analytically, by considering the standing upper cutoff mode to have an amplitude that is weakly nonlinear and slowly varying in space and time (neglecting higher harmonics), it is readily shown that the amplitude obeys a damped parametrically driven nonlinear Schrödinger equation [2], which has the stable single-kink solution

$$\theta_n(t)=2(-1)^n\left[\frac{\gamma}{3\alpha}\right]^{1/2}\tanh\left[\left[\frac{\gamma}{2c^2}\right]^{1/2}(n-x_0)\right]\times\cos(\omega t+\delta)\,, \tag{2}$$

where $\gamma=\omega_1^2-\omega^2+\nu$, $\nu=(\eta^2/4-\omega^2\beta^2)^{1/2}$, and

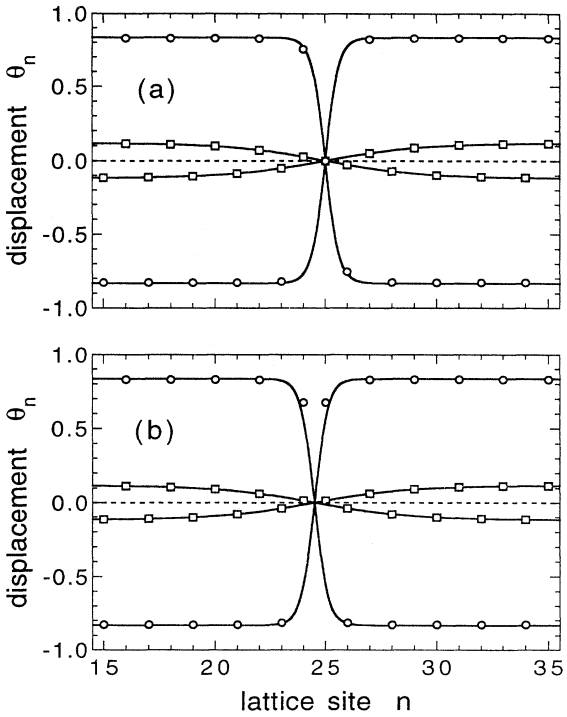

FIG. 1. (a) Antisymmetric and (b) symmetric kinks in the upper cutoff mode at turning points of the motion. The points, which correspond to the lattice sites, are numerical; the curves are analytical (NLS theory). The lattice contains 49 sites (not all are shown). The drive parameters are $\omega=1.1832$ and $\eta=0.074$ in the smaller-amplitude cases and 0.9875 and 0.200, respectively, in the larger-amplitude cases.

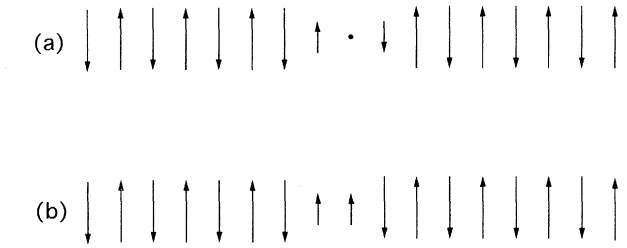

FIG. 2. Diagrammatic representations of highly localized upper cutoff kinks: (a) antisymmetric state, and (b) symmetric state.

$\tan(2\delta)=\omega\beta/\nu$. The lattice spacing is assumed to be unity, x_0 is the location of the node, and the linear frequency of the upper cutoff mode is $\omega_1=(\omega_0^2+4c^2)^{1/2}$. Curves of (2), in which the lattice site n is replaced by a continuous variable, are shown with the numerical data in Fig. 1. The theory agrees extremely well with the small-amplitude data. This agreement persists with the antisymmetric kink data [Fig. 1(a)] even when the amplitude is neither weakly nonlinear nor slowly varying. This appears to be coincidental because the theory for these parameters disagrees substantially (roughly 20%) with the symmetric data [Fig. 1(b)] in the kink region. Also in contrast to the theory is that the phases of the oscillators (to a 180° difference) in each steady state are not all exactly the same, although the variation is slight (roughly a 0.05° lag in the kink region). The phase in the uniform regions agrees well the theoretical value δ in (2), which predicts a value of 36.80° in the low-amplitude case and 8.62° in the high-amplitude case. The error is 0.70° in the latter case, and half this in the former.

Figure 3 shows the regions in the drive parameter plane in which the upper cutoff mode and antisymmetric kink exist and are stable. There are 50 sites in the lattice with the pure mode, and 49 sites in the lattice with the

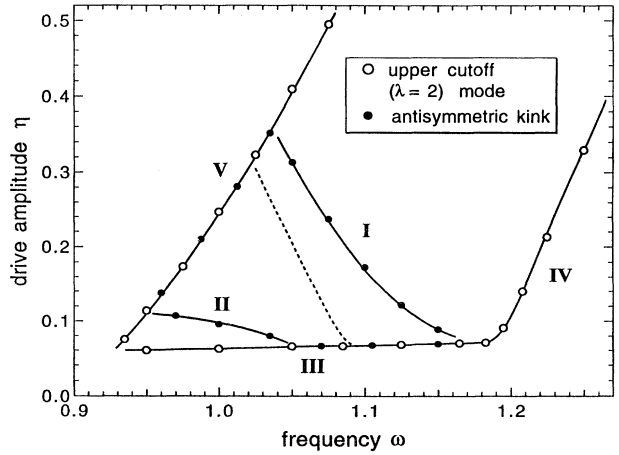

FIG. 3. Drive parameter plane boundaries of the upper cutoff mode (open circles) and antisymmetric kink (closed circles). The linear frequency of the mode is $\omega_1=1.1832$. The dashed curve is explained in Sec. VI.

kink. The stability was tested by random perturbations, as stated in Sec. II. The boundaries of the regions were determined by a painstaking process of finely incrementing a drive parameter, waiting for a steady state to be attained, and then checking the stability. As the drive amplitude or frequency is slowly increased, a remarkable transformation occurs along boundary I. The kink undergoes a structural change from the antisymmetric to the symmetric state. This involves a spontaneously broken symmetry; the kink translates one-half of a lattice spacing to either the right or left. The instability along boundary II corresponds to the onset of quasiperiodic motion in the kink region. The additional frequency in the motion corresponds to a relatively slow decrease in phase and increase in amplitude in one-half of the kink region, while the opposite occurs in the other half. The process reverses, and then repeats indefinitely. The symmetry reversals and quasiperiodicity are examined in more detail in Sec. VI, along with the influence of the effective Peierls-Nabarro potential which arises due to the energy difference between kink states of definite symmetry.

Along boundaries III and IV in Fig. 3, both the kink and pure mode decay to rest. The decay initiates from a nonzero response amplitude along III, and from an essentially zero response amplitude along IV. This is precisely what the theory predicts for a single oscillator whose natural frequency is ω_1. Boundary III corresponds to the relationship $\eta=2\omega\beta$, for which the radicand ν in γ in (2) vanishes. Here the system is "falling off the end" of the frequency response curve [19], which is inherently bent to smaller frequencies in the case of parametric excitation of a softening system. Boundary IV corresponds to the Mathieu parametric excitation threshold curve for frequencies greater than the linear frequency of the mode. For weak drive and dissipation, and for drive frequencies that do not substantially depart from the linear modal frequency ω_1, the Mathieu curve is given by

$$\eta^2=4(\omega_1^2-\omega^2)+4\omega^2\beta^2 \ . \tag{3}$$

(This expression is slightly more accurate than the standard one [19] which is a hyperbola in η and ω, because we have not made the final explicit approximation that the values of ω and ω_1 are close to each other.) Near boundary IV the kink occupies the entire lattice, and becomes a linear mode which has a sinusoidal spatial variation. Boundary V corresponds to the uninteresting instability in which the oscillators are displaced "over the top" of the external potential wells [$|\theta|>\omega_0/\alpha^{1/2}$ in (1)], resulting in divergent motion. In the region above boundary IV, kinks exist but their symmetry is indefinite. For example, if an antisymmetric kink in this region is perturbed, the final location of the node is in general neither a lattice site nor halfway between lattice sites. If the kink state is again perturbed, the node will in general change its location. This behavior is not unexpected as the linear response region is approached, because there is no preference for the location of the node in the linear limit. It is interesting that this lack of symmetry occurs even though the kinks are still localized; the lack of symmetry appears to be the first indication of the approach to the linear response region in the parameter plane.

This continuous connection between a kink state and a linear mode is the key to our physical understanding of these localized states. It is simpler to first examine the case of a lower cutoff hardening kink. We consider an undamped undriven lattice that possesses a hardening lower cutoff mode, e.g., a lattice described by (1) where $\beta=0$, $\eta=0$, and $\alpha<0$. For simplicity, free boundary conditions are assumed. The fundamental (lower cutoff) mode has uniform amplitude. We begin with the next small-amplitude (linear) mode, which has a node at the center of the lattice and antinodes at the ends, and a sinusoidal profile. We now imagine increasing the amplitude and ask how the profile changes such that every oscillator has the same frequency and is either in phase or 180° out of phase; i.e., such that the response is a mode of the system. Simply scaling the sinusoid violates this, because the nonlinearity causes the frequency in the regions of the antinodes to increase but does not alter the frequency in the region of the node. Furthermore, if the profile remains sinusoidal the coupling does not alter the frequency anywhere in the lattice. To achieve a modal response, we must modify the sinusoid profile such that there is a local balance of the effects of nonlinearity and coupling (or curvature of the profile) upon the frequency. This is accomplished in two ways: by flattening the profile in the antinodal region, thus reducing the frequency there because the contribution due to coupling is reduced, and by increasing the curvature of the profile in the nodal region, thus increasing the frequency there because the contribution due to coupling is increased. With these deformations, it is possible to imagine that all of the oscillators will have a common frequency and phase. The critical fact that we learn from observations is that the profile can readily become practically uniform in the antinodal region, so that the nodal region is no longer influenced by boundary conditions. When this happens, it is no longer appropriate to consider the state as the first mode above the lower cutoff mode, but as a localized kink in the lower cutoff mode. The kink is free to move as a result of external perturbations or nonuniformity, and thus acts as a particle.

The argument for upper cutoff softening kinks, which are those that are investigated in this article, is similar to the argument above. The difference is that, whereas increasing the curvature of a lower cutoff mode causes an *increase* in frequency, increasing the curvature of an upper cutoff mode causes a *decrease* in the frequency. This evidently must be the case because the linear mode just below the upper cutoff mode has a frequency less than the upper cutoff frequency. Alternatively, a qualitative examination of the actual coupling force leads to the same conclusion [5].

Analytically, the approximate description of the transition from a sinusoidal envelope to a localized hyperbolic tangent envelope is the elliptic sn function [3,5]. In the limit of the hyperbolic state the kinks are solitons [11].

IV. NONCUTOFF KINKS

Kinks are not restricted to cutoff modes, but can also occur in noncutoff modes. We have observed these in

many modes whose wavelengths are either an even or odd number of lattice spacings. Figure 4 shows an example of a symmetric kink in the wavelength-four mode in which every other site is a node. This kink corresponds to a 90° spatial phase mismatch between the pure-mode domains on either side of it. As shown in Fig. 4(b), the temporal phases of the antinodes reveal a small deviation in the kink region. The phases of the quasinodes approach a constant value for oscillators sufficiently far from the localized structure. By performing simulations with a larger number of lattice sites and with kinks of greater localization, we have established that this leveling off of the phases is not a boundary effect [although it appears to be in Fig. 4(b)]. It is interesting that the phases of the quasinodes are substantially less localized than the amplitudes.

Whereas cutoff kinks correspond to only one possible mismatch in spatial phase between the two extended domains, many mismatches are possible in the case of noncutoff modes. The structures of noncutoff kinks are therefore much more varied than those of cutoff kinks. Examples are shown in Figs. 5(b)–5(e), which display some of the simpler kinks that can occur in the wavelength-four mode in which every other lattice site is a node [Fig. 5(a)]. As in the cutoff case, only kinks with definite symmetry are observed to be stable, unless their amplitude is small (see below). Symmetric and antisymmetric kinks corresponding to the same spatial phase mismatch are paired in Fig. 5. The kinks in Figs. 5(b)–5(d) are "elementary" in the sense that they are the simplest structures that exist for a particular mismatch. More complicated kinks can exist for the same mismatch and drive parameters. For example, some initial conditions lead to a steady-state juxtaposition of the two kinks in Fig. 5(b) such that the mismatch is that in Fig. 5(c). As another example, the kinks in Fig. 5(e) correspond to *no* mismatch between the two domains, and so the most elementary state in this case is no kink (i.e., the pure mode). Note that these kinks can be obtained by a local perturbation of the pure mode, in contrast to the elementary kinks. The antisymmetric kink in Fig. 5(e) can clearly be considered as a juxtaposition of two out-of-phase symmetric kinks in Fig. 4(c). The symmetric kink in Fig. 5(e) appears to be most simply considered as two elementary domain walls (Sec. V) bounding an upper cutoff domain.

Another indication of the greater complexity of noncutoff kinks compared to the cutoff case is that the kink energy (Sec. VI) does not have the same sign for all kinks. The energy of the cutoff kinks is always negative. The noncutoff kinks in Fig. 5(b) have negative energy, whereas those in Fig. 5(d) have positive energy. The energy of the symmetric kink in Fig. 5(c) is positive, while the energy of its antisymmetric partner is negative.

Figure 6 shows the drive parameter plane regions in

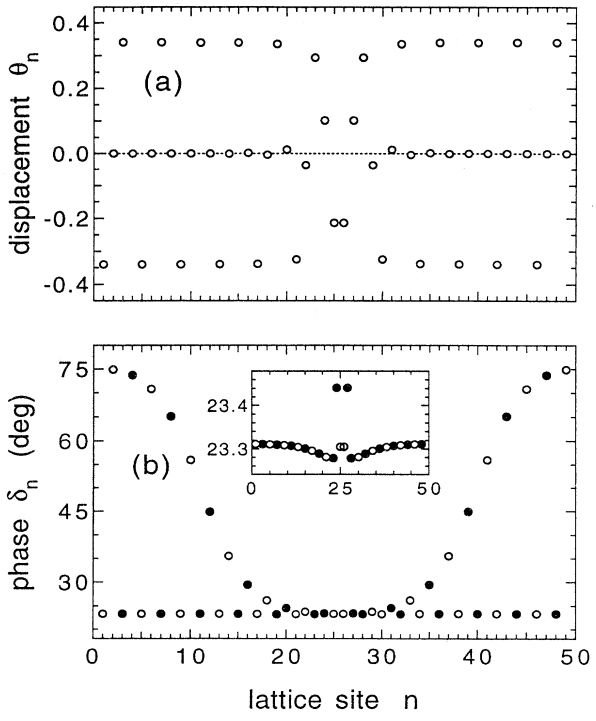

FIG. 4. A symmetric kink in the wavelength-four mode: (a) signed amplitudes of the oscillators, and (b) phases. The closed and open circles in (b) represent a phase difference of 180°. The drive parameters are $\omega=1.07$ and $\eta=0.09$.

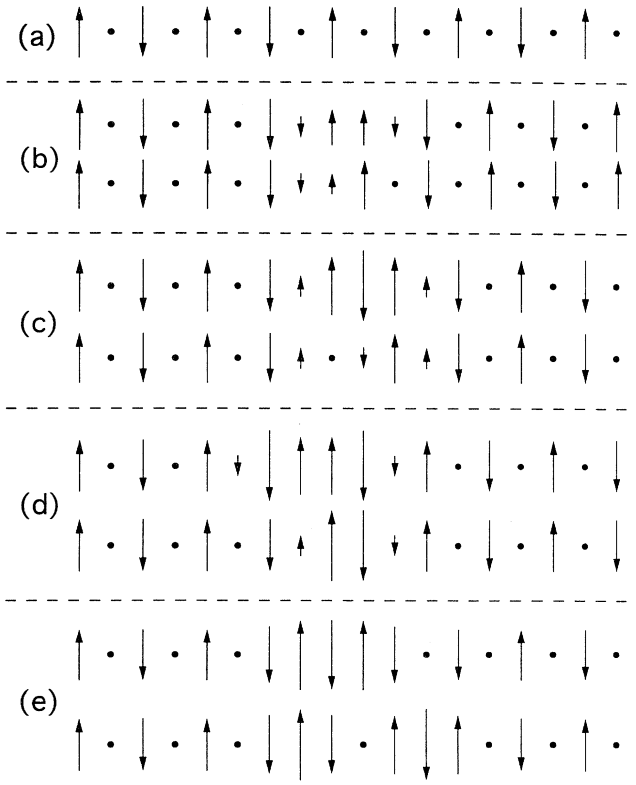

FIG. 5. (a) Pure wavelength-four mode, and (b)–(e) various kinks in this mode. Each pair corresponds to the same spatial phase mismatch between the two uniform domains, but to opposite symmetry. The kinks in (b) and (d) correspond to ±90° mismatches, the kinks in (c) to a 180° mismatch, and the kinks in (e) to no (or a 360°) mismatch.

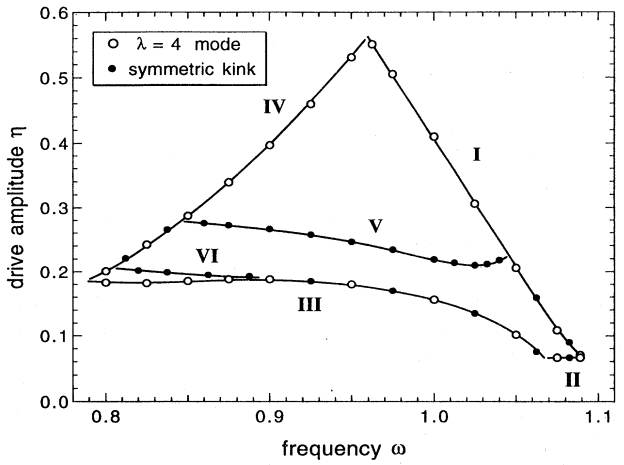

FIG. 6. Drive parameter plane boundaries of the wavelength-four mode (open circles) in Fig. 5(a), and the symmetric kink (closed circles) in Fig. 5(b). The linear frequency of the mode is $(\omega_0^2+2c^2)^{1/2}=1.0954$.

which the pure wavelength-four mode in Fig. 5(a) and the symmetric kink in Fig. 5(b) exist and are stable. There are 52 sites in the lattice with the pure mode, and 49 sites in the lattice with the kink. As stated in Sec. II, the stability of the states was tested by imposing random perturbations of the amplitudes. The instabilities in the pure mode itself are interesting. Along boundary I in Fig. 6, the nodes develop out-of-phase motion relative to each other, at the same frequency of the antinodes. The final state along the lower half of this boundary is the wavelength-four mode in which the nodes lie halfway between pairs of lattice sites. Along the upper half of the boundary, the motion diverges. Along boundary II, the system decays to rest. Along boundary III, the nodes develop in-phase motion relative to each other. For dimensionless frequencies greater than about 1.0, the motion is chaotic as evidenced by the scatter of points in Poincaré maps and by the broadening of peaks in fast-Fourier transforms. For smaller frequencies along this boundary, as well as for all frequencies along boundary IV, the motion diverges. We conclude that most of the instabilities of the pure noncutoff mode unexpectedly do *not* correspond to those of a single oscillator, whereas all of the instabilities of the pure upper cutoff mode (Sec. III) correspond to a single oscillator. The pure noncutoff mode acts as a single oscillator only along the short boundary II and the uninteresting boundary IV.

The symmetric kink exists in a subset of the pure-mode region in Fig. 6, as a result of two mechanisms. Along boundary V, the kink acts as a nucleation site for the instability that occurs along boundary I for the pure mode, causing the boundary to occur at lower drive amplitudes. Along the left half of boundary V the motion diverges, and along the right half quasiperiodicity develops in the kink region. Along boundary VI the motion sometimes diverges, and at other times exhibits a symmetry reversal similar to that for the upper cutoff kink (Sec. III). In most of the kink drive plane region, the state occupies few lattice sites, as represented in Fig. 5(b). However, in the vicinity of the linear frequency (lower right corner), the kink spreads out and diminishes in amplitude. Furthermore, under perturbation the kink in general loses its symmetry, as would occur for a linear wave. Very near the corner, the kink occupies the entire lattice, and becomes the linear normal mode whose eigenfrequency is nearest and less than the linear frequency of the wavelength-four mode.

The physical qualitative reasoning of the connection between localized noncutoff kink states and extended linear modes is not as strong as in the upper cutoff case (Sec. III). The reasoning does not yield continuum noncutoff kinks, but at most a periodic chain of either cutoff kinks and antikinks or breathers and antibreathers. For lattices where the wavelength of the motion is not large compared to the lattice spacing, the emergence of a localized kink in the high-amplitude limit of a linear mode can be physically understood from the condition of uniform frequency and phase (Sec. III) for at least certain simple cases. The general validity of this reasoning, however, is an open question.

V. DOMAIN WALLS

Whereas kinks connect two domains of the *same* wave number, domain walls connect two domains of *different* wave number. An example is shown in Fig. 7. Domain walls are stable localized structures that are inherently

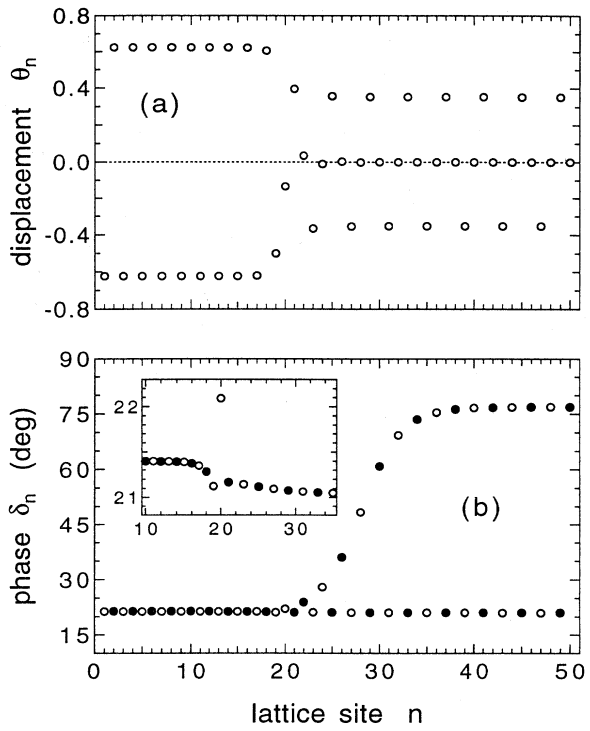

FIG. 7. Elementary domain wall between the wavelength-two (upper cutoff) and wavelength-four modes: (a) signed amplitudes of the oscillators, and (b) phases. The closed and open circles in (b) represent a phase difference of 180°. The drive parameters are $\omega=1.07$ and $\eta=0.10$.

nonlinear; in contrast to kinks, domain walls are not connected to linear modes and are thus genuine new degrees of freedom. There is a small temporal phase difference (0.4° in this case) between the antinodes in the two domains on either side of the domain wall. This occurs because the phase relative to the drive is identical to that of the corresponding pure mode, and the phases of the two pure modes are slightly different. We were motivated to check this to determine whether the two domains were phase locked. If this were the case, then the domain wall would not be a truly localized structure; in the limit of a large number of lattice sites from the domain wall one would still be able to distinguish whether or not this structure were there. As in the case of noncutoff kinks in the wavelength-four mode (Sec. IV), the phases of the quasinodal oscillators approach a constant as the distance from the domain wall is increased, and the phases are not as localized as the amplitudes.

As with kinks, domain walls can exist at any of a discrete set of locations one lattice spacing apart. Furthermore, the domain wall structure is not unique for fixed values of drive parameters, but depends upon the initial conditions. The "elementary" state in Fig. 7 or Fig. 8(a) appears to be unique: All other domain walls we have observed occupy a greater number of lattice sites, and can be interpreted as a bound state of the elementary domain wall and a kink. An example of such a "complex" state is shown in Fig. 8(b). This can be viewed as a bound state of an elementary domain wall and a kink in the wavelength-four mode [specifically, the symmetric kink in Fig. 5(b)], or alternatively as a kink in the wavelength-two (upper cutoff) mode and an elementary domain wall. We have observed many such complex domain walls corresponding to various types of symmetric and antisymmetric kinks in the wavelength-four and wavelength-two modes. Domain walls of greater complexity have also been observed.

We have also observed domain walls between modes other than the wavelength-two and wavelength-four, including longer-wavelength modes that are quasicontinuous. The current continuum theory [13,14] of domain walls predicts that these states do *not* exist in the continuum limit of the lattice described by the equation of motion (1). The resolution of this contradiction may be that the theory assumes that the response in each domain is only weakly nonlinear, whereas the numerical data show a strongly nonlinear response [14].

That the juxtaposition of a kink and elementary domain wall forms a bound state is dramatically exhibited by the state in Fig. 8(c), which is composed of the antisymmetric kink in Fig. 5(b) and the elementary domain wall. For the drive parameters $\omega=1.025$ and $\eta=0.20$ this state is stable. However, for the same drive parameters the isolated kink state is *unstable.* The proximity of the elementary domain wall acts to stabilize the structure in a manner that is not yet understood, to our knowledge.

Figure 9 shows the regions in the drive parameter plane in which there exist the pure wavelength-two and wavelength-four modes (refer to Fig. 3 and Fig. 6, respectively), and the steady-state elementary domain wall [Fig. 8(a)]. There are 50 sites in the lattice with the domain wall, and reflecting boundary conditions are used. The stability was checked as in the previous cases. The region of the elementary domain wall is nearly identical to the overlap region of the two pure modes. The exception occurs as the lower right corner is approached: As the domain wall occupies a greater number of lattice sites, it eventually undergoes a structural transformation into the complex state represented in Fig. 8(b). We refer to this process, in which the structure of a localized state spontaneously transforms into a more complicated localized structure, as "complexification." The instability is highly hysteretic and, not surprisingly, the time-averaged lattice energy (Sec. VI) is found to be discontinuous across the instability. The complexification appears to be a consequence of the lack of a linear mode corresponding to the domain wall: The structure can only occupy a larger number of lattice sites by introducing a kink bound to the elementary domain wall.

A necessary condition for the existence of a domain wall is that the drive parameter plane regions of the two pure modes overlap. The data in Fig. 9 suggest that this condition may also be sufficient. Because the linear

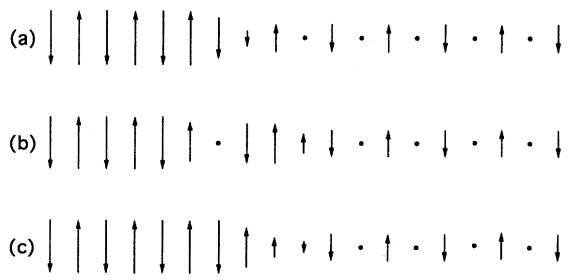

FIG. 8. Domain walls between the wavelength-two (upper cutoff) and wavelength-four modes: diagrammatic representations of a highly localized (a) elementary domain wall, (b) complex domain wall, and (c) different complex domain wall.

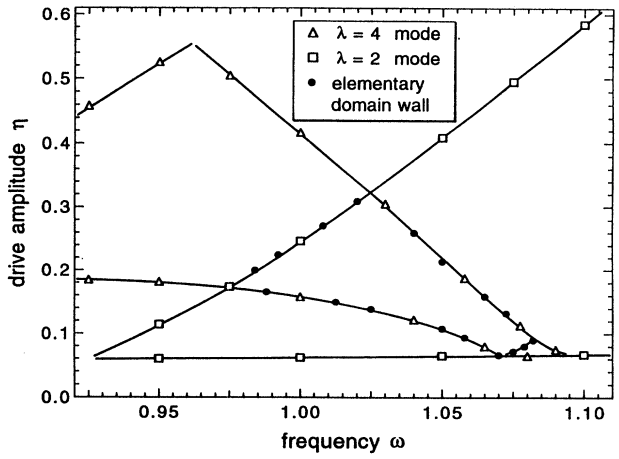

FIG. 9. Drive parameter plane boundaries of the upper cutoff mode (open squares), wavelength-four mode (open triangles), and elementary domain wall (closed circles) between these two modes.

modal frequency spacing decreases for smaller values of the coupling parameter c^2, the amount of overlap is greater, which accounts for our choice of a small value ($c^2=0.1$). Indeed, for $c^2=1$ we are unable to obtain a steady-state domain wall between the wavelength-two and -four modes. This is consistent with the fact that the drive parameter regions for the pure modes in Fig. 9 can easily be shown to have no overlap when $c^2=1$, if we make the plausible assumption that a change in the value of the coupling parameter only shifts the regions by a frequency equal to the change in the linear modal frequency. Domain walls should exist for $c^2=1$ if the difference of the wave numbers of the two extended modes is sufficiently small.

VI. SYMMETRY REVERSALS, QUASIPERIODICITY, AND CHAOS

To have a single quantity that characterizes the kinks, we consider their energy. The natural preliminary definition is that the kink energy equals the energy of the lattice with one kink minus the energy of the lattice without the kink, in which both states have the same drive parameters. The lattice must of course consist of a sufficiently large number N of oscillators compared to the number occupied by the kink such that the kink energy is independent of N. There are several problems with the definition, however. First, the instantaneous mechanical energy (kinetic plus potential) of a driven damped nonlinear oscillator in the steady state is *not* constant in time. (This is a genuine effect which is not related to the numerical finite-difference artifact in which the energy oscillates an amount that scales with the time step.) The oscillation is easily removed by averaging over one cycle of the motion. The time-averaged total energy of a lattice with N sites is

$$E=\left\langle \sum_{n=1}^{N} \varepsilon_n(t) \right\rangle_t , \tag{4}$$

where the bracket subscript denotes the quantity over which the average is performed, and where the instantaneous energy of the nth lattice site is

$$\varepsilon_n(t)=\frac{1}{2}\left[\frac{d\theta_n}{dt}\right]^2+\frac{\omega_0^2}{2}\theta_n^2-\frac{\alpha}{4}\theta_n^4 + \frac{c^2}{4}[(\theta_{n+1}-\theta_n)^2+(\theta_n-\theta_{n-1})^2] . \tag{5}$$

The coupling energy has been chosen to be half of that between sites n and $n+1$, and half of that between sites n and $n-1$. The second problem is that the number of oscillators in a lattice with one kink cannot equal the number in a lattice without the kink, when periodic boundary conditions are employed. We overcome this by averaging the energy of the pure mode over the lattice sites in one wavelength, in addition to time averaging. This yields the average energy per lattice site

$$\varepsilon=\langle \varepsilon_n(t) \rangle_{t,n} . \tag{6}$$

The kink energy is then

$$E_{\text{kink}}=E-N\varepsilon , \tag{7}$$

where E is the time-averaged energy (1) of the lattice with the kink, N is the number of sites in this lattice, and ε is the average energy (6) per lattice site of the pure mode.

The kink energy offers a means of quantifying the symmetry reversals (Secs. III and IV). Figure 10 shows a hysteresis loop of the upper cutoff kink energy vs frequency for a fixed drive amplitude, as the frequency is slowly and monotonically changed. The upper data correspond to the symmetric kink, and the lower data to the antisymmetric kink. The curves are the symmetric and antisymmetric kink energies according to the nonlinear Schrödinger (NLS) theory. The antisymmetric kink energy curve agrees well with the numerical data, whereas the symmetric kink energy curve does not. The discrepancy is a result of the inaccuracy of the theory in the symmetric kink region (Sec. III). The numerical data reveal that the down-jump occurs where the energy is stationary with respect to frequency. This is known to occur in simpler systems, for example, a driven damped nonlinear oscillator or extended standing wave mode in the hysteretic regime.

In a Hamiltonian lattice, the stability of a localized state is dictated by its energy as a function of position. If the lattice is nonintegrable, this energy is invariably an extremum for states of definite symmetry (i.e., symmetric or antisymmetric), and gives rise to an effective Peierls-Nabarro (PN) potential [20–23]. Only the state of minimum energy is stable. Our observations show that drive and dissipation can fundamentally alter this. In a range of drive parameters, *both* states of definite symmetry are stable under small perturbations. Moreover, in another range of drive parameters, only the state of *greater* energy is stable. The generalization of the PN potential to include drive and dissipation is an open question.

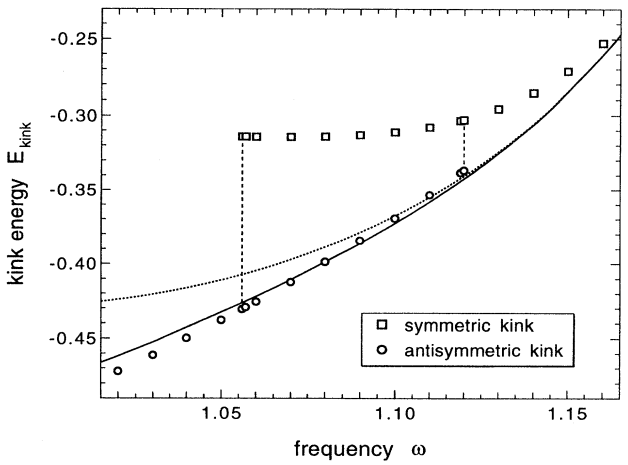

FIG. 10. Hysteresis loop of the upper cutoff kink energy as a function of frequency, for a fixed drive amplitude of $\eta=0.125$. The points are numerical; the curves are analytical (NLS theory). The solid curve corresponds to the antisymmetric kink, and the dotted curve to the symmetric kink. The jumps are indicated by dashed lines.

As stated in Secs. III and IV, upper cutoff and noncutoff kinks develop quasiperiodic (QP) motion for certain ranges of the drive parameter values. The QP motion occurs in the kink region and, in the case of the antisymmetric kink, causes the site that was the node to oscillate. We thus refer to this oscillator as the "quasinode." QP motion is typically associated with mode competition. It is interesting that here the additional frequency corresponds to a variation of the response that oscillates from one side of the quasinode to the other. Figures 11(a) and 11(b) show the motion of oscillators nearby and far from the quasinode during the QP motion of an upper cutoff kink. The QP period for the drive parameters in this case is between 11 and 12 periods of the primary motion. The QP motion is clearly associated with the localized structure: The relative amount of this motion decreases with distance from the kink, and it does not occur for the pure mode.

Phase plays a fundamental role in the onset of QP motion and in the motion itself. The instability involves a phase decrease of the oscillators on one side of the quasinode and a phase increase on the other side. The decrease causes the oscillators to absorb energy and thus increase in amplitude, while the increase causes the oscillators to lose energy and thus decrease in amplitude. The process continues until some limitation causes it to reverse. Figure 11(c) shows the time dependence of the energy of the lattice on one side of the quasinode (including half the energy of the quasinodal oscillator), compared to half of the total energy. The energies are averaged over one drive cycle because the instantaneous energy oscillates a relatively large amount. Although the total energy is not constant, the oscillations of the energy of the half-lattice are proportionally much larger. To confirm that energy is actually passing from one side to the other, rather than varying solely as a direct result of the external drive, we have computed the average power flow across the quasinode and the average power flow from the external drive to half of the lattice. For the drive parameters in Fig. 11, we have found that the flow across the quasinode and the external drive contribute roughly equally to the oscillation of the energy of the half-lattice.

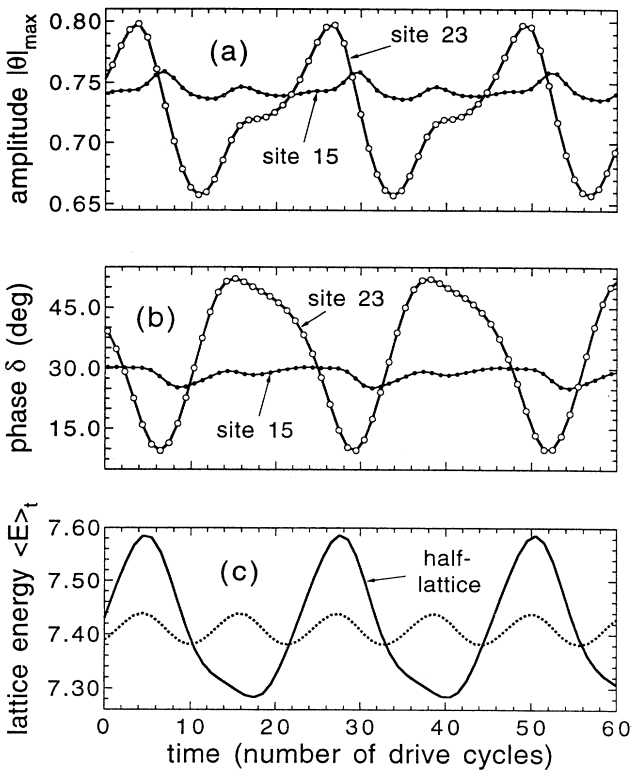

FIG. 11. Quasiperiodic motion of an upper cutoff kink in which the quasinode is located at site 25: Time dependence of the (a) amplitudes of site 23 (open circles) and 15 (closed circles), (b) corresponding phases, and (c) energy of the left half of the lattice (solid curve) and half the energy of the entire lattice (dotted curve). The amplitudes and phases were measured during each cycle of the drive, and the energies were averaged over each cycle of the drive. The drive parameters are $\omega=1.0$ and $\eta=0.075$.

The QP motion of the symmetric kink in the wavelength-four mode is similar to that of the upper cutoff kink. We expect that this motion is observable in other kinks and has similar properties. We have also observed QP motion in a domain wall.

As the upper cutoff kink is driven deeper into the QP regime in the drive parameter plane in Fig. 3, the motion eventually becomes chaotic as evidenced by the scatter of points in Poincaré maps and the broadening of peaks in fast-Fourier transforms. The amount of chaotic motion relative to the regular motion decreases with distance from the quasinode, as shown in the Poincaré maps in Fig. 12. A crude measure of the relative amount of chaos in the Poincaré map is the area of the smallest upright rectangle that bounds the points. The values of this area are displayed with the maps in Fig. 12. The area decreases roughly exponentially from the quasinode, with an exponential coefficient of 0.3 per lattice spacing. A similar state of localized chaos has recently been investigated [24]. However, this state is complicated by the fact that it occurs between two domain walls, and so the region of chaos can for fixed drive parameters span an arbitrarily long region of the lattice. The chaotic upper cutoff kink reported here may offer a simpler state in which localized chaos can be probed. Indeed, we believe that the chaotic upper cutoff kink is the limit of the state in Ref. [24] as the chaotic region of the lattice is reduced to its minimum size.

VII. FEW-DEGREE-OF-FREEDOM MODELS OF THE INSTABILITIES

As stated in Sec. III, boundary I in the drive parameter plane in Fig. 3 corresponds to an instability in which the upper cutoff kink undergoes a transformation from an antisymmetric to symmetric state as either the drive frequency or drive amplitude is slowly increased. In particular, the node of the antisymmetric kink becomes unstable. It is natural to wonder whether this instability can be simply understood as a single oscillator parametrically driven at the threshold of excitation. We can then predict where the instability should occur in the drive pa-

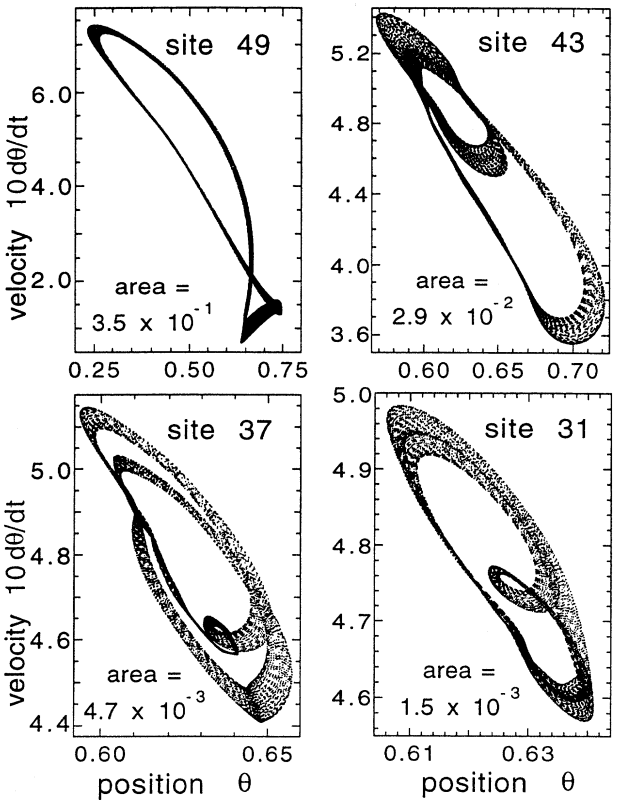

FIG. 12. Chaotic motion of an upper cutoff kink in which the quasinode is at site 50 of a 99-site lattice: Poincaré maps of lattice sites 49, 43, 37, and 31. The areas of the rectangles that bound the points are displayed. The drive parameters are $\omega=0.96$ and $\eta=0.073$.

rameter plane if we assume that the oscillators nearest the nodal oscillator always have equal-and-opposite displacements (as in the steady antisymmetric kink state). In this case, the net coupling force on the nodal oscillator is the same as if the nearest-neighbor oscillators are at rest. The frequency of the nodal oscillator in the limit of small amplitudes is thus neither the uncoupled frequency ω_0 nor the linear upper cutoff frequency ω_1, but is identical to the linear frequency of the wavelength-four mode. According to this single-oscillator model, then, the drive amplitude threshold for the antisymmetric kink instability is determined by replacing ω_1 in the Mathieu threshold relationship (3) with $(\omega_0^2+2c^2)^{1/2}$. The resultant left half of the curve is shown dashed in Fig. 3. The actual instability (boundary I) lies substantially to the right of this curve. The failure of the single-oscillator model is due to the assumption of equal-and-opposite displacements of the nearest-neighbor oscillators. This is evidently *not* the case; these oscillators (and others) must respond to perturbations of the nodal oscillator such that there is a stiffening of the frequency, causing the instability to shift to the right. The instability thus involves a collective effect associated with the oscillators in the region of this localized structure. It should also be noted that the single-oscillator model completely fails to predict the instability along boundary II in Fig. 3, where quasiperiodicity develops in the antisymmetric kink region.

The two oscillators nearest the center of a symmetric kink have equal instantaneous displacements. The noncutoff kink in Fig. 4 is an example. If we consider a system of two linearly coupled identical softening nonlinear oscillators, it can be shown that the symmetric mode parametrically drives the antisymmetric mode, and that excitation of the latter can occur depending upon the drive parameters. The resultant Mathieu curve for excitation of the antisymmetric mode is skewed to lower frequencies in this case because the mode is excited in the presence of the symmetric mode. As in the single-oscillator model above, it is natural to wonder here if the instabilities exhibited by symmetric kinks can be modeled by this two-oscillator system. The symmetric noncutoff kink in Fig. 4 is particularly suited for an investigation of this possibility because the oscillators nearest to the symmetric pair have small amplitudes in most of the drive parameter plane Fig. 6. In particular, these amplitudes are small along the instabilities marked by boundaries V and VI in this plane. For example, for $\omega=0.95$ and $\eta=0.24$ (near the middle of boundary V), the amplitude is 3.4% of the amplitude of the symmetric pair. We thus model this state by assuming that the two outer oscillators are nodes. We have calculated and numerically investigated the instabilities of this two-oscillator model. Although boundary V in Fig. 6 lies remarkably close to the instability in the model, there is a fundamental problem. The symmetric state in the model is stable *above* the boundary, whereas the symmetric kink is stable *below* the boundary. We conclude that the lattice instability is fundamentally altered by the small motion of the nearest neighbors and the ability of these oscillators (and others) to move independently when the symmetric kink is perturbed. That is, the collective nature of the motion cannot be ignored. As in the model of the antisymmetric kink above, it should be noted that the two-oscillator model completely fails to predict the instability along boundary VI in Fig. 6.

Few-degree-of-freedom models similar to those investigated above can also be developed for other kinks. It is suspected that the models will also fail in these cases as a result of the collective motion of the oscillators.

VIII. CONCLUSIONS

With a highly interactive and visual computer simulation program, we have investigated various structural properties of standing upper cutoff kinks, noncutoff kinks, and domain walls in a damped parametrically driven lattice. These modes are nonlinear self-localized states that can occur at any of a discrete set of locations of the lattice. The properties include preferential kink symmetry, a variety of distinct noncutoff kink states corresponding to different initial conditions and spatial mismatches, a variety of distinct domain wall states corresponding to different initial conditions, and spontaneous hysteretic transitions as the drive parameters are slowly varied. The robust nature of these localized structures in different numerical lattices and a physical lattice

suggest that they may occur in many other systems, and may have similar properties. A nonlinear Schrödinger theory approximately describes the steady-state upper cutoff kinks, although these states can exist at amplitudes beyond which the perturbation theory is valid. Our quasicontinuum observations of domain walls contradict the current theory of these states.

By mapping boundaries of the region in the drive parameter plane in which the steady-state localized structures exist, we have observed instabilities which lead to symmetry reversals and complexifications, as well as the onset of localized quasiperiodicity and chaos. Furthermore, we have observed that the kinks are continuously connected to linear modes of the system. The drive plane region corresponding to the quasilinear motion of the states is very small compared to the region of nonlinear motion. Domain walls are inherently nonlinear states, and thus lead to the fact that the number of modes of the system greatly exceeds the number of degrees of freedom.

The observations in this article point to the need for further analytical studies of the damped driven kinks and domain walls, including an understanding of preferential symmetry and the various instabilities. The effective Peierls-Nabarro potential of the underlying Hamiltonian system is fundamentally inadequate to explain the preferential symmetry here. Plausible few-degree-of-freedom models of the instabilities fail, indicating collective behavior that may be particular to mesoscopic systems. We have mapped the drive parameter planes for only several of the localized states, and for only single values of the coupling and damping parameters. It is likely that further investigations of the localized states reported here will reveal additional phenomena.

ACKNOWLEDGMENTS

We are grateful for discussions with B. Galvin, A. Greenfield, A. Larraza, and S. Putterman. The work of one of us (B.D.) was supported in part by the Office of Naval Research, and the work of the other (W.W.) by the Office of Basic Energy Science, Department of Energy.

[1] R. K. Dodd, J. C. Eilbeck, J. D. Gibbon, and H. C. Morris, *Solitons and Nonlinear Wave Equations* (Academic, London, 1982), pp. 1–5.

[2] Bruce Denardo, Brian Galvin, Andrés Larraza, Alan Greenfield, Seth Putterman, and William Wright, Phys. Rev. Lett. **68**, 1730 (1992).

[3] Bruce Denardo, William Wright, Seth Putterman, and Andrés Larraza, Phys. Rev. Lett. **64**, 1518 (1990).

[4] J. Wu, R. Keolian, and I. Rudnick, Phys. Rev. Lett. **52**, 1421 (1984); J. Wu and I. Rudnick, Phys. Rev. Lett. **55**, 204 (1985).

[5] Bruce Denardo, Ph.D. dissertation, Department of Physics, University of California, Los Angeles, California, 1990 (unpublished).

[6] Mary Atchley, M.S. thesis, Department of Physics, Naval Postgraduate School, Monterey, California 1992 (unpublished).

[7] A. Larraza and S. Putterman, J. Fluid Mech. **148**, 443 (1984).

[8] J. Miles, J. Fluid Mech. **148**, 451 (1984).

[9] N. Grønbeck-Jensen, Yuri S. Kivshar, and M. R. Samuelsen, Phys. Rev. B **43**, 5698 (1991).

[10] Kazuyoshi Yoshimura and Sihinuke Watanabe, J. Phys. Soc. Jpn. **60**, 82 (1991).

[11] V. E. Zakharov and A. B. Shabat, Zh. Eksp. Teor. Fiz. **61**, 118 (1971) [Sov. Phys. JETP **34**, 62 (1972)]; V. E. Zakharov and A. B. Shabat, Zh. Eksp. Teor. Fiz. **64**, 1627 (1973) [Sov. Phys. JETP **37**, 823 (1973)].

[12] Yuri S. Kivshar and Sergei K. Turitsyn, Phys. Lett. A **171**, 344 (1992); Yuri S. Kivshar, Phys. Rev. B **46**, 8652 (1992); Phys. Rev. Lett. **70**, 3055 (1993); Phys. Lett. A **173**, 172 (1993).

[13] Bruce Denardo, Andrés Larraza, Seth Putterman, and Paul Roberts, Phys. Rev. Lett. **69**, 597 (1992).

[14] Seth Putterman and P. H. Roberts, Proc. R. Soc. London Ser. A **440**, 135 (1993).

[15] Yuri S. Kivshar, Angel Sánchez, and Luis Vázquez, Phys. Rev. A **45**, 1207 (1992).

[16] Yuri S. Kivshar, Niels Grønbeck-Jensen, and Mogens R. Samuelsen, Phys. Rev. B **45**, 7789 (1992).

[17] V. Muto, P. S. Lomdahl, and P. L. Christiansen, Phys. Rev. A **42**, 7452 (1990).

[18] Ref. [1], pp. 505–506.

[19] L. D. Landau and E. M. Lifshitz, *Mechanics,* 3rd ed. (Pergamon, New York, 1976), pp. 80–83, 90–92.

[20] Michel Peyrard and Martin D. Kruskal, Physica D **14**, 88 (1984).

[21] Oleg Braun, Oksana A. Chubykalo, Yuri Kivshar, and Luis Vázquez, Phys. Rev. B **48**, 3734 (1993).

[22] Yuri Kivshar and David K. Campbell, Phys. Rev. E **48**, 3077 (1993).

[23] Thierry Dauxois and Michel Peyrard, Phys. Rev. Lett. **70**, 3935 (1993).

[24] Alan Greenfield, Seth Putterman, and William Wright, Phys. Lett. A **185**, 321 (1994).